Chemical Engineering Journal 385 (2020) 123892

Contents lists available at ScienceDirect

Chemical Engineering Journal

journal homepage: www.elsevier.com/locate/cej

A new family of actinide sorbents with more open porous structure: Fibrous functionalized silica microspheres

Li-Yong Yuan[a], Ge Gao[a,b], Chuan-Qi Feng[b], Zhi-Fang Chai[a,c], Wei-Qun Shi[a,*]

[a] Laboratory of Nuclear Energy Chemistry, Institute of High Energy Physics, Chinese Academy of Sciences, Beijing 100049, China
[b] Hubei Collaborative Innovation Center for Advanced Organic Chemical Materials & Ministry-of-Education Key Laboratory for Synthesis and Applications of Organic Functional Molecules, Hubei University, Wuhan 430062, China
[c] Engineering Laboratory of Advanced Energy Materials, Ningbo Institute of Industrial Technology, Chinese Academy of Sciences, Ningbo, Zhejiang 315201, China

HIGHLIGHTS

- A new family of actinide sorbents with more open porous structure was developed.
- The sorbents show clear U(VI) sorption at pH as low as 2.5.
- The sorbents showed good stability and reusability.
- Radiation stability of the sorbents was evaluated with comparison with existing sorbents.

GRAPHICAL ABSTRACT

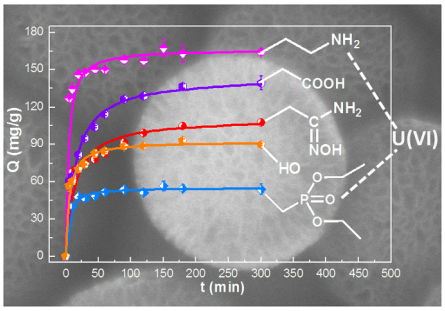

ARTICLE INFO

Keywords:
Fibrous mesoporous silica microsphere
Functionalization
Open porous structure
U(VI)
Solid sorption

ABSTRACT

No one could have failed to notice the fact that the basic research on the separation of nuclear fuel associated radionuclides is currently a hot topic as a result of the universality of nuclear industry. Herein, a kind of fibrous mesoporous silica microspheres and its derivatives tailored by amine (APS-F-SiO_2), carboxyl (COOH-F-SiO_2), phosphate (DPTS-F-SiO_2) and amidoxime (AD-F-SiO_2), respectively, were successfully fabricated for high efficient U(VI) capture from aqueous solution. The synthesized sorbents were well characterized by SEM, FT-IR, N_2 sorption-desorption measurement and TGA, which confirms achievement of the functionalization. The U(VI) sorption onto these microsphere sorbents was then explored in detail. The results clearly show that these microsphere materials especially APS-F-$SiO_2$and COOH-F-SiO_2 are indeed effective U(VI) sorbents, in terms of considerable sorption capacity of ~200 mg/g, the short equilibrium time of less than 30 min, the ionic strength-independent nature, and desirable selectivity towards U(VI) over a range of competing ions. Moreover, the sorbed U(VI) ions can be easily desorbed from the sorbents by controlling a lower pH, e.g. pH 1.0, and the reclaimed sorbent can be reused without obvious reduction of U(VI) uptake even after 4 sorption-desorption cycles, implying an excellent stability and reusability of the sorbents. These sorbents also keep high performance in U(VI) sorption even following 400 kGy gamma irradiation in water, which further highlights the opportunity for this kind of materials in radionuclide separation. The finding of the present work offers new platform for developing actinide sorbents applied in various practical cases.

* Corresponding author.
E-mail address: shiwq@ihep.ac.cn (W.-Q. Shi).

https://doi.org/10.1016/j.cej.2019.123892
Received 8 November 2019; Received in revised form 16 December 2019; Accepted 19 December 2019
Available online 21 December 2019

1. Introduction

The massive expansion of industry has led the world to face the challenge of energy crisis, which arouses a wide concern on nuclear energy due to its efficient, clean and low cost advantages [1]. Development of nuclear energy, however, should pay much attentions to environmental problems related to radionuclides [2,3]. In particular, as the main fuel of nuclear reactors, the separation and recovery of uranium is of great practical significance. In the last decades, plenty of novel techniques [4–9] were explored to detect and eliminate uranium (typically occurs as U(VI)) from aqueous solution, among which solid phase extraction (SPE) is becoming one of the most prevailing techniques because of its superiorities such as less or even no organic solvent, small changes of pH in sorption process, simple equipment, easy safe operation and low-cost [10–12]. With the continuous development of solid phase extraction [13–20], mesoporous silica-based materials [21–26], such as MCM-41, SBA-15, and KIT-6 [27], have been widely concerned as U(VI) sorbents, a result of their specific advantages of large surface area, big pore size, and extremely chemical stability. To be successful in such an application, however, the mesoporous silicas require modification by organic functional groups to improve selectivity and efficiency. A review contributed by Frank Hoffmann et al. [28] on the topic of functional modification of mesoporous materials has been published, in which a series of methods for successful preparation of functional materials were summarized. A great number of papers have also published to expand the research about the work of nuclide sorption based on mesoporous silicas. Wang and coworkers [29], for example, opened up the synthesis of luminescent mesoporous silica-carbon dots called CDs/SBA-NH_2 for actinide sorption. In situ monitoring of the sorption process was achieved in this work. Li and coworkers [30] prepared functionalized magnetic mesoporous silica nanoparticles for U(VI) removal from low and high pH groundwater. Recently, we published a series of works on U(VI) and Th(IV) capture by using functionalized mesoporous silicas [13,22–24,31], in which several mesoporous materials as effective actinide sorbents were confirmed in view of fast sorption rate, large sorption capacity, desirable selectivity towards U(VI) or Th(IV), and ionic strength independence nature. Due to the limitations of the pore size of the conventional mesoporous materials, however, the incorporation of functional groups especially bulky ligands always results in the problem of pore clogging and poor mass transfer. Fibrous mesoporous silica microspheres (F-SiO_2) represent a new family of mesoporous materials with more open porous structure, which thus offers a vast opportunity to overcome this problem. The first example of F-SiO_2 (KCC-1) was reported by Polshettiwar et al. [32], which are featured with excellent physical properties of high surface area, unprecedented fibrous surface morphology, high thermal (up to 950 °C) and hydrothermal stabilities, and high mechanical stability. More importantly, the more open porous structure in this kind of materials not only allow modification of more and bulky functional groups but also facilitate transmission and diffusion of molecular and/or ions in it. Since being first reported in 2010, F-SiO_2 materials have been widely used in extraction of biomacromolecules [33], separation [21], and drug delivery [34]. To the best of our knowledge, however, utility of this kind of materials on the sorption of actinides such as U(VI) has been rarely reported.

In this work, a series of functionalized fibrous mesoporous silica microspheres prepared by post-grafting 3-aminopropyltrimethoxysilane (APS-), carboxyl (COOH-), diethylphosphatoethyl-triethoxysilane (DPTS-) and amidoxime (AD-), respectively, were explored as U(VI) sorbents. The aims of this work are to develop more applicable and effective U(VI) sorbents and offer new manners and opportunities for solid phase extraction of actinides from waste water. To achieve these aims, the sorption of U(VI) by pristine F-SiO_2 and its grafted derivatives have been investigated under various conditions of pH, sorption time, initial U(VI) concentrations, and ionic strength. Selectivity test, regeneration of the sorbents, and evaluation of radiation stability were also performed for practical application considerations.

2. Experimental

2.1. Materials

Tetraethoxysilane (TEOS) and (2-cyanoethyl) triethoxysilane (CETEOS, 97%) was purchased from Meryer, China. Cetyltrimethylammo-nium bromide (CTAB) was obtained from SCRC, China. Cyclohexane, urea, isopropyl alcohol (IPA), anhydrous ethanol, sulfuric acid, diethylphosphatoethyltriethoxysilane (DPTS), N-[3-(triethoxysilyl)propyl]-4,5-dihydroimidazole (DIM), hydroxylammonium chloride ($NH_2OH{\cdot}HCl$), aqueous ammonia, sodium carbonate anhydrous, and 3-aminopropyltrimethoxysilane (APS) were purchased from Meryer, China. Uranyl nitrate hexahydrate ($UO_2(NO_3)_2{\cdot}6H_2O$, ACS grade) was purchased from Merck, Germany. All these materials were used as received. Standard stock solution (1.45 g L^{-1}) of U(VI) was prepared by dissolving the appropriate amounts of $UO_2(NO_3)_2{\cdot}6H_2O$ in deionized water. All other chemicals were of analytical grade and used without further purification. Deionized water used in all experiments was obtained from the Milli-Q water purification system.

2.2. Synthesis of the sorbents

2.2.1. Synthesis of fibrous mesoporous silica microspheres

1.0 g of CTAB and 0.6 g of urea were dissolved in 30 mL distilled water, which was stirred for 2 h at 303 K. And then 30 mL of cyclohexane and 0.92 mL of IPA were added into the solution subsequently under vigorous stirring. After 2 h, 2.5 mL of TEOS were added dropwise, followed by a 30 min stirring at 303 K. The mixture was transferred to oil-bath and heated to 343 K for 15 h. The solid product, named as F-SiO_2, was collected after centrifugation, thrice washing with distilled water and ethanol, respectively, and drying at 323 K.

2.2.2. Synthesis of phosphonate, and amino functionalized F-SiO_2

In a typical synthesis of phosphonate functionalized F-SiO_2, 0.3 g of the prepared F-SiO_2 and 150 μL of DPTS were dissolved in 25 mL anhydrous ethanol, then 50 μL of aqueous ammonia was added drop by drop. The mixture was transferred to oil-bath and heated to 343 K for 12 h. The solid product, termed as DPTS-F-SiO_2, was collected after centrifugation, thrice washing with distilled water and ethanol, respectively, and drying in a blast oven at 323 K. Amino functionalized F-SiO_2, termed as APS-F-SiO_2, was prepared following the same procedure as that used for DPTS-F-SiO_2, except that 3-aminopropyltrimethoxysilane (APS) was used instead of diethylphosphatoethyltriethoxysilane (DPTS) during the synthesis.

2.2.3. Synthesis of carboxyl functionalized F-SiO_2

0.2 g of the prepared F-SiO_2 and 500 μL of cyanoethyl (CETEOS) were dispersed in 25 mL anhydrous ethanol. Then 50 μL of sulfuric acid was added, and the mixture was heated to 343 K for 12 h. The solid phase product, termed as COOH-F-SiO_2, was collected after centrifugation, thrice washing with distilled water and ethanol, respectively, and drying in a blast oven at 323 K.

2.2.4. Synthesis of amidoxime functionalized F-SiO_2

(1) 0.3 g of F-SiO_2 and 400 μL of CETEOS were dispersed in 25 mL anhydrous ethanol. Then 50 μL of aqueous ammonia was added. The mixture was heated to 343 K for 12 h. The mid product of cyano-modified material was obtained after centrifugation, thrice washing with distilled water and ethanol, respectively, and drying in a blast oven at 323 K. (2) Under nitrogen atmosphere, 1.5 g of $NH_2OH{\cdot}HCl$ was dissolved in 24 mL of distilled water under magnetic stirring at room temperature, followed by the addition of 1.1 g of Na_2CO_3 (solution 1). 0.5 g of the as-synthesized cyano-modified material was dispersed in 24 mL of distilled water (solution 2). Then, the solution 2 was added

dropwise into the solution 1. The mixture was heated to 343 K for 3 h. The final product, termed as AD-F-SiO_2, was obtained after centrifugation, thrice washing with distilled water and ethanol, respectively, and drying in a blast oven at 323.

2.3. Analytical techniques

The synthesized samples were characterized by scanning electron microscopy (SEM), N_2 sorption-desorption isotherm experiments, thermogravimetric analytical (TGA) and Fourier transform infrared spectroscopy (FTIR). The residual concentration in supernatants of U (VI) in all the experiments and other tested ion(s) in the selectivity test were determined by inductively coupled plasma optical emission spectroscopy (ICP-OES). Detailed illustrations were listed in the Supporting Information (SI-1).

2.4. Sorption experiments

All the sorption experiments were performed using batch method at room temperature. The initial concentrations of U(VI) varied from 5 to 200 ppm. The pH of solutions was adjusted by adding inappreciable volumes of diluted nitric acid or sodium hydroxide. In a typical sorption experiment, 4 mg of sorbents was kept in contact with 10 mL of U(VI) solution in a beaker. After stirring for 5 h at room temperature, the two phases were separated by centrifugation for 10 min with a speed of 8000 rpm. Then the concentrations of U(VI) in the aqueous solution were determined by the inductively coupled plasma optical emission spectroscopy (ICP-OES). The control experiment was performed at the same time by using the identical U(VI) solution in the absence of the sorbents. The solid–liquid experiment was repeated at least three times for each adsorption data with the uncertainty within 5%. Detailed illustrations were listed in the Supporting Information (SI-2)

3. Results and discussion

3.1. Characterizations of the sorbents

The fibrous morphology of the prepared silica microspheres, i.e. F-SiO_2, APS-F-SiO_2, COOH-F-SiO_2, AD-F-SiO_2 and DPTS-F-SiO_2, is shown in Fig. 1a. The SEM images indicate that all the samples possess ordered spherical fiber structure with a diameter of 300–400 nm. The FTIR spectra of the prepared silica microspheres are compared in Fig. 1b and Fig. S1. For F-SiO_2, the main absorption band of Si–O stretching (1100 cm^{-1}), Si–O–Si bending (800 cm^{-1}), and Si-OH bending (945 cm^{-1} and 1630 cm^{-1}) are clearly observed. After functionalization by organic groups, the absorption band of saturated C–H stretching caused by –CH_3 and –CH_2 groups appears at 2930 cm^{-1} and 2860 cm^{-1}, respectively. Meanwhile, the absorption of C═O stretching vibration (1575 cm^{-1}) for COOH-F-SiO_2, N–H stretching vibration (3425 cm^{-1}) for APS-F-SiO_2 and C═N stretching vibration (1670 cm^{-1}) for AD-F-SiO_2 are clear indications that the expected functional groups were successfully incorporated. For DPTS-F-SiO_2, unfortunately, it is difficult to distinguish the absorption bands assigned to phosphonate, i.e. P═O and P-O-R stretching mode, from being submerged in the main peak of the siloxane. The N_2 sorption-desorption isotherms of both F-SiO_2 and grafted F-SiO_2 microspheres (Fig. 1d) are found to be type IV, typical for a mesoporous material. Table 1 lists the specific surface area and pore volume of all the prepared silica microspheres. It can be seen that the introduction of a variety of functional groups results in a general decrease in both the specific surface area and the total pore volume of the produced SiO_2 microspheres, which is well in agreement with the case of reported functionalization of conventional mesoporous silicas, e.g. SBA-15 [13]. The pore size distributions of all the silica microspheres were also derived by Barrett–Joyner–Halenda (BJH) method using the adsorption branch of the isotherm, as shown in Fig. 1e. Unlike conventional mesoporous silicas, the fibrous silicas microspheres, including the grafted

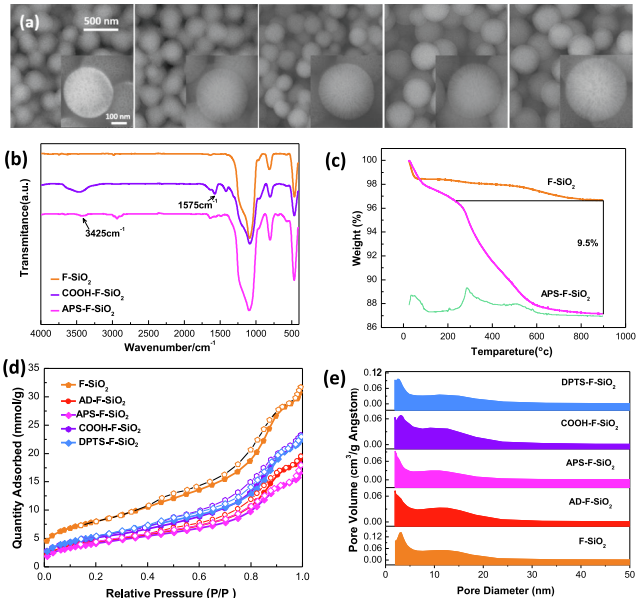

Fig. 1. Characterizations of the sorbents. (a) SEM images (from left to right: F-SiO_2, DPTS-F-SiO_2, APS-F-SiO_2, AD-F-SiO_2, COOH-F-SiO_2. (b) FTIR spectra. (c) TGA profiles. (d) N_2 sorption-desorption isotherms. (e) Pore size distribution.

Table 1
The specific surface area and total pore volume of pristine and modified F-SiO_2.

Materials	BET surface area (m^2 g^{-1})	Pore volume (cm^3 g^{-1})
F-SiO_2	675	1.2
APS-F-SiO_2	346	0.5
COOH-F-SiO_2	417	0.8
DPTS-F-SiO_2	443	0.7
AD-F-SiO_2	358	0.6

samples, possess larger pores of 10–20 nm besides the pores of 2–5 nm. The larger pore size is more suitable for subsequent modification and mass transfer of metal ions, thus facilitate sorption application. In addition, to determine the degree of modification in the fibrous mesoporous silicas, thermal analysis was performed in the temperature range of 25–900 °C. The results are provided in Fig. 1c and Fig S2. For the pristine F-SiO_2, less than 4% weight loss occurs in the whole temperature range, being reasonably attributed to the pyrolysis of the exposed silanol groups on the surface. For the four grafted materials, the weight loss with the increasing temperature presents three distinct stages, corresponding to the volatilization of physically adsorbed solvent below 200 °C, the pyrolysis of the attached organic groups on the pore surface at temperature range of 200–400 °C, and the pyrolysis of the attached functional groups inside the pores above 400 °C, respectively. Nearly 800 °C, the TGA profiles reach a plateau, and the total weight loss of the four grafted F-SiO_2, i.e. APS-F-SiO_2, COOH-F-SiO_2, AD-F-SiO_2 and DPTS-F-SiO_2 except the volatilization of solvent are about 9.5%, 11.8%, 26.4% and 8.5%, respectively, from which the coverage of functional group in the four materials can be calculated to be 1.6 mmol g^{-1}, 1.6 mmol g^{-1}, 3.0 mmol g^{-1} and 0.5 mmol g^{-1}, respectively (the molecular mass of APS-, COOH-, AD- and DPTS- functional groups are 59 u, 74 u, 88 u and 166 u, respectively). Considering all of the above results, it is apparent that the expected fibrous functionalized mesoporous materials have been successfully prepared.

3.2. U(VI) sorption in pristine F-SiO_2 and modified F-SiO_2

To compare the sorption capabilities of modified F-SiO_2 with pristine F-SiO_2, sorption of U(VI) from aqueous solution into those materials were performed at various conditions.

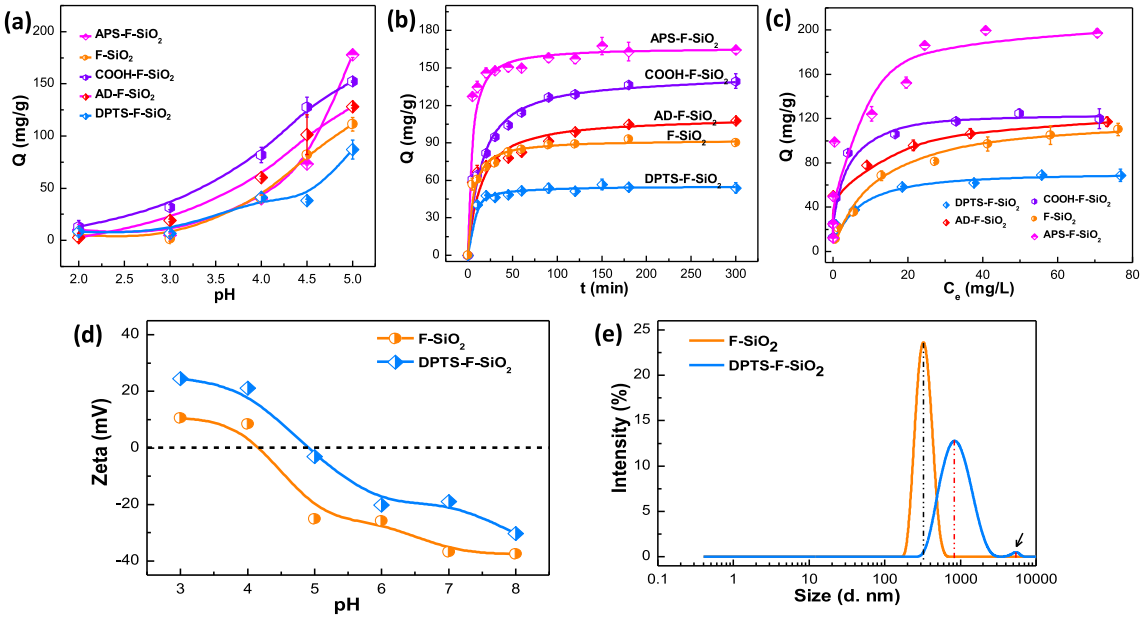

Fig. 2. (a) pH-dependent U(VI) sorption in pristine and modified F-SiO_2. $m_{sorbent}/V_{solution}$ = 0.4 mg mL^{-1}, $[U]_{initial}$ = 100 mg L^{-1}; (b) Sorption kinetics of U(VI) by pristine and modified F-SiO_2. pH = 5 ± 0.02, $m_{sorbent}/V_{solution}$ = 0.4 mg mL^{-1}, $[U]_{initial}$ = 100 mg L^{-1}. The points are experimental date, while the solid lines are the fitting results by pseudo-second-order kinetic model.); (c) Sorption isotherm of U(VI) by pristine and modified F-SiO_2. pH = 5 ± 0.02, $m_{sorbent}/V_{solution}$ = 0.4 mg mL^{-1}. (The solid lines are the fitting results by Langmuir isotherm model); (d) Zeta potentials of DPTS-F-SiO_2 as function of pH compared with pristine F-SiO_2; (e) Particle size distribution of DPTS-F-SiO_2 compared with pristine F-SiO_2.

3.2.1. Effect of pH

Solution pH is a significant influential parameter for metal ion sorption, because it remarkably affects the form of metal ions as well as the surface charge and binding sites of sorbent. Herein, U(VI) sorption by pristine F-SiO_2 and modified F-SiO_2 at pH ranging from 2 to 5 was performed to explore the effect of pH. As shown in Fig. 2a, the sorption of U(VI) by all the materials rapidly increases with the augmentation of solution pH. At pH 2.0, for example, almost no U(VI) sorption occurs for all the materials, whereas at pH 5.0, the sorption capacities reach 111 mg g^{-1}, 178 mg g^{-1}, 152 mg g^{-1}, 128 mg g^{-1}, and 87 mg g^{-1} for F-SiO_2, APS-F-SiO_2, COOH-F-SiO_2, AD-F-SiO_2, and DPTS-F-SiO_2, respectively. Such a pH-dependent sorption can be understood based on the surface charge of the sorbents. That is, a lower pH results in a positively charged surface of the sorbents, and the electrostatic repulsion effect hinders the sorption of positively charged U(VI) ions. At a higher pH, the electrostatic repulsion effect decreases or even disappears due to the deprotonation of the sorbents. The coordination or hydrogen bond interactions incite an increase of U(VI) sorption. Besides, pH-induced U(VI) speciation (see SI-5 and Fig. S3 in the Supporting Information) could also be responsible for the pH-dependent sorption. With increasing of pH, U(VI) species transform gradually from free UO_2^{2+} to multi-nuclear hydroxide complexes such as $(UO_2^{2+})_3(OH)_5^{+}$. These complexes may be more favored by the sorbents, thus leading to a higher U(VI) sorption. Whatever, taking into account all these factors, pH = 5 was selected for further sorption experiments. At this pH, the modified F-SiO_2 sorbents except DPTS-F-SiO_2 show superior U(VI) uptake compared to pristine F-SiO_2, suggesting an important role of functional groups on binding U(VI) ions. Besides, it is worth noting that COOH-F-SiO_2 show clear U(VI) sorption at pH as low as 2.5, probably due to its negatively or less positively charged surface and strong coordination ability of carboxyl groups, which make it a promising sorbent for actinide extraction from acidic solution.

3.2.2. Sorption kinetics

The sorption rate of U(VI) onto F-SiO_2, DPTS-F-SiO_2, APS-F-SiO_2, AD-F-SiO_2, COOH-F-SiO_2 was investigated by covering different contact time of 1 min to 300 min at an initial U(VI) concentration ($[U]_{initial}$) of 100 mg L^{-1}. As shown in Fig. 2b, the sorption of U(VI) onto all the materials is ultra-fast in the initial 5 min, and then the sorption process becomes slow until an equilibrium reaches at *ca.* 60 min. The sorption rate is faster than that in some porous sorbents, such as 20 h in MCM-41 [35], 24 h in nanoporous carbon [36] and 24 h in multiwalled carbon nanotubes grafted with carboxymethyl cellulose [37], which can be reasonably attributed to more open porous structure in the fibrous microspheres. To clarify the sorption process, the pseudo-first-order kinetic model and the pseudo-second-order kinetic model were applied to analyze the sorption data. The detailed description of the two models and the fitting results are presented in SI-6 and Table S1 in the Supporting Information. It is apparent that for all the materials, the pseudo-second-order kinetic model matches well with the sorption data, giving a much better correlation coefficient (R^2 > 0.99) than that for the pseudo-first-order kinetic model. That is, the pseudo-second-order model is more appropriate to explain the kinetics of U(VI) sorption onto these fibrous microspheres, implying that the sorption process is mainly dominated by a chemical sorption. It is known that ordinary exchange processes is rapid and controlled mainly by diffusion [38], whereas for a chelating exchanger the process is relatively slow and controlled either by a particle diffusion or by a chemical reaction [39]. In the case of the fibrous SiO_2 microspheres, more open porous structure allows a fast diffusion of U(VI), while functional group on the surface of the microspheres behave like a chelating exchanger. Both effects result in a fast chemical sorption process. Whatever, to ensure the complete sorption of U(VI), the mixture of the sorbents and the solution was stirred for at least 5 h in subsequent experiments.

3.2.3. Sorption isotherms

The amount of U(VI) sorbed in pristine F-SiO_2 and functionalized F-SiO_2 as a function of U(VI) concentration in supernatant at the equilibrium state (C_e), i.e. sorption isotherm, was determined at a constant pH of 5.0 ± 0.02 by altering the initial U(VI) concentrations from 5 to 200 mg L^{-1}. The data were shown in Fig. 2c. It is clear that U(VI) uptake by both pristine and modified F-SiO_2 has a sharp increase at C_e < 20 mg L^{-1}, corresponding to ca. 59 mg g^{-1}, 90 mg g^{-1}, 97 mg g^{-1}, 112 mg g^{-1}, 173 mg g^{-1} of U(VI) sorption onto DPTS-F-

SiO_2, F-SiO_2, AD-F-SiO_2, COOH-F-SiO_2, APS-F-SiO_2, respectively, after which the sorption reaches an equilibrium. All the modified F-SiO_2 except DPTS-F-SiO_2 show superior U(VI) sorption over pristine F-SiO_2, implying the important roles of the functional groups for binding U(VI). The lower U(VI) sorption by DPTS-F-SiO_2 can be rationalized from the surface properties point of view. That is, phosphonate group exhibits stronger hydrophobicity and makes the material be prone to cohesion. The cohesion reduces exposure of the sorbent to U(VI) solution, thus decreases the U(VI) loading. This proposal can be supported by the following experimental facts. First, the zeta potentials of DPTS-F-SiO_2 as function of pH (Fig. 2d) suggest that the surface of SiO_2 microspheres following phosphonate modification becomes near electroneutral at pH 5, which generally results in the cohesion of sorbent particles. Second, the comparison of particle size distributions of F-SiO_2 and DPTS-F-SiO_2 (Fig. 2e) show that DPTS-F-SiO_2 has a much larger particle size than pristine F-SiO_2, clearly revealing the cohesion of DPTS-F-SiO_2 particles. To analyze the sorption mode of U(VI) onto the fibrous silica microspheres, the sorption data were fitted by Langmuir and Freundlich models. The detailed descriptions of the two models as well as the fitting plots are presented in the supporting information (SI-7) and the parameters are given in Table 2. It is found that the Langmuir model well matches ($R^2 > 0.98$) with the experimental data for all the sorbents, suggesting a monolayer and uniform sorption nature of U(VI) onto these materials. This result is in good agreement with our expectation that U(VI) ions are sorbed mainly through complexation with the functional groups on surface of the sorbents. For pristine F-SiO_2, the residual silanol group is believed to serve as an O-donor ligand for complexation with U(VI) ions, thus leading to a reasonable U(VI) sorption.

3.3. Further practical concerns

Effects of ionic strength and competing ions on the U(VI) sorption onto these fibrous silica microspheres as well as reusability and radiation stability of the sorbents were further assessed in view of possible applications of this kind of material in U(VI) (or other radioactive nuclides) uptake from wastewater.

Effect of ionic strength The effect of ionic strength on the sorption of U(VI) onto F-SiO_2, APS-F-SiO_2, and COOH-F-SiO_2 were investigated in the presence of $NaClO_4$ with concentrations varying from 0 to 0.2 mol L^{-1}. The results are shown in Fig. 3a. For APS-F-SiO_2 and COOH-F-SiO_2, the U(VI) uptake almost kept constant with rising concentration of $NaClO_4$ ([$NaClO_4$]), suggesting an ionic strength independent sorption process. It has been reported that U(VI) was sorbed dominantly as inner-sphere complexes when the sorption is independent of the ionic strength.[40] Accordingly, the ionic strength independent process here indicates that U(VI) formed inner-sphere complexes on the surface of APS-F-SiO_2 and COOH-F-SiO_2, which once again supports the expectation that U(VI) ions are sorbed mainly through complexation with the functional groups on surface of the sorbents. For pristine F-SiO_2, however, an increased U(VI) uptake occurred at high ionic strength, which is a less common observation. We rationalize this abnormal observation as follows: due to the lack of functional groups, ion exchange (when positively charged surface of the sorbent) or electrostatic interactions (when negatively charged surface of the sorbent) contributes to a substantial proportion of U (VI) sorption on F-SiO_2. As the ionic strength (i.e. the concentration of $NaClO_4$) increased, the contribution of ion exchange/electrostatic interaction is enhanced by the more readily ion exchange between U(VI) and Na^+ or the stronger electrostatic interaction between U(VI) and ClO_4^-, thus leading to an increased U(VI) uptake. Whatever, given that the salt concentration is very high in wastewater, the ionic strength effects here are clear advantage for the application of this kind of material in wastewater cleaning or recovery of U(VI) from wastewater.

Competitive sorption of U(VI) To evaluate the selectivity of APS-F-SiO_2 and COOH-F-SiO_2 towards U(VI), the competitive sorption of U (VI) by APS-F-SiO_2 and COOH-F-SiO_2 from the aqueous solution containing a range of competing metal ions, including Co^{2+}, Gd^{3+}, La^{3+}, Nd^{3+}, Ni^{2+}, Sm^{3+}, Sr^{2+}, Yb^{3+}, Zn^{2+}, were performed at pH 5 ± 0.01, in which the concentration of all the metal ions was identical as 0.65 mmol L^{-1}. As shown in Fig. 3b, under the test conditions, the U(VI) uptake in APS-F-SiO_2 and COOH-F-SiO_2 is more than 130 mg g^{-1} and 80 mg g^{-1}, respectively, while the uptake of all other metal ions is less than 10 mg g^{-1}. It is known that selectivity coefficient is always used to evaluate the selectivity of a sorbent for a particular metal ion. Herein, the selectivity coefficient ($S_{U/M}$) for U(VI) relative to competing ions is defined as [41]:

$$S_{U/M} = \frac{K_d^U}{K_d^M}$$

where K_d^U and K_d^M are the distribution ratio of U(VI) and competing ions in sorbent and solution, respectively. It is found that at pH 5 the $S_{U/M}$ value for U(VI) relative to all the competing ions is more than 15 and 13 for APS-F-SiO_2 and COOH-F-SiO_2, respectively. The results confirm the desirable selectivity of the F-SiO_2 sorbents towards U(VI) ions over a range of competing metal ions.

Regeneration and reuse of the sorbents From the perspective of low-cost applications, regeneration and reuse of sorbent must be considered. Herein, the desorption of U(VI) from APS-F-SiO_2 was performed using HNO_3 solution as eluent. The experiment details are shown in Supporting Information **SI-8**. We found that the sorbed U(VI) can be easily desorbed from APS-F-SiO_2 by HNO_3 solution, and the desorption rate clearly enhanced with the increasing of the concentration of HNO_3 ([HNO_3]). When [HNO_3] reached 0.1 M, a complete recovery (> 99%) of the sorbed U(VI) was achieved. As mentioned above, the U(VI) sorption by APS-F-SiO_2 is pH dependent. Almost no sorption of U(VI) onto APS-F-SiO_2 occurred at lower pH. Accordingly, the desorption of U(VI) from APS-F-SiO_2 can be illustrated as a cation exchange between protons and the U(VI) ions. To further assess the stability of the APS-F-SiO_2 sorbent during U(VI) sorption and desorption, the reusability of APS-F-SiO_2 was tested by repeating sorption–desorption cycle, and the results was shown in Fig. 3c. As can be seen that the U(VI) uptake onto APS-F-SiO_2 was not distinctly decreased even after four sorption–desorption cycles, which manifests excellent reusability of the sorbent. Moreover, it is noteworthy that during each sorption–desorption cycle, 0.1 mol L^{-1} HNO_3 solution was used as the eluent, and the sorbent was dried at 100 °C. The repeated acid-treatment process and heat-treatment process did not incite discernible changes in the sorbent, affording further evidence that the APS-F-SiO_2 sorbent possesses good stability for real applications.

Table 2
The fit results from the Langmuir and Freundlich equations.

Isotherm model							
Langmuir				Freundlich			Saturation capacity from experiment (mg g^{-1})
materials	Q_m (mg g^{-1})	b (mL mg^{-1})	R^2	K_F (mg g^{-1})	n	R^2	
F-SiO_2	122	0.1037	0.98	17	2.1	0.97	110
APS-	208	0.2526	0.98	106	6.9	0.85	197
COOH-	125	0.6061	0.99	58	5	0.90	120
AD-	127	0.1558	0.99	51	5.1	0.98	117
DPTS-	72	0.2593	0.99	26	4.1	0.97	69

3.4. Sorption stability under gamma irradiation

To be successful in the applications of radioactive nuclides capture, the sorbents should be at least relatively robust to high radiation doses. Herein, irradiation test of pristine F-SiO_2 and APS-F-SiO_2 was performed, in which dry samples and samples soaked in water were

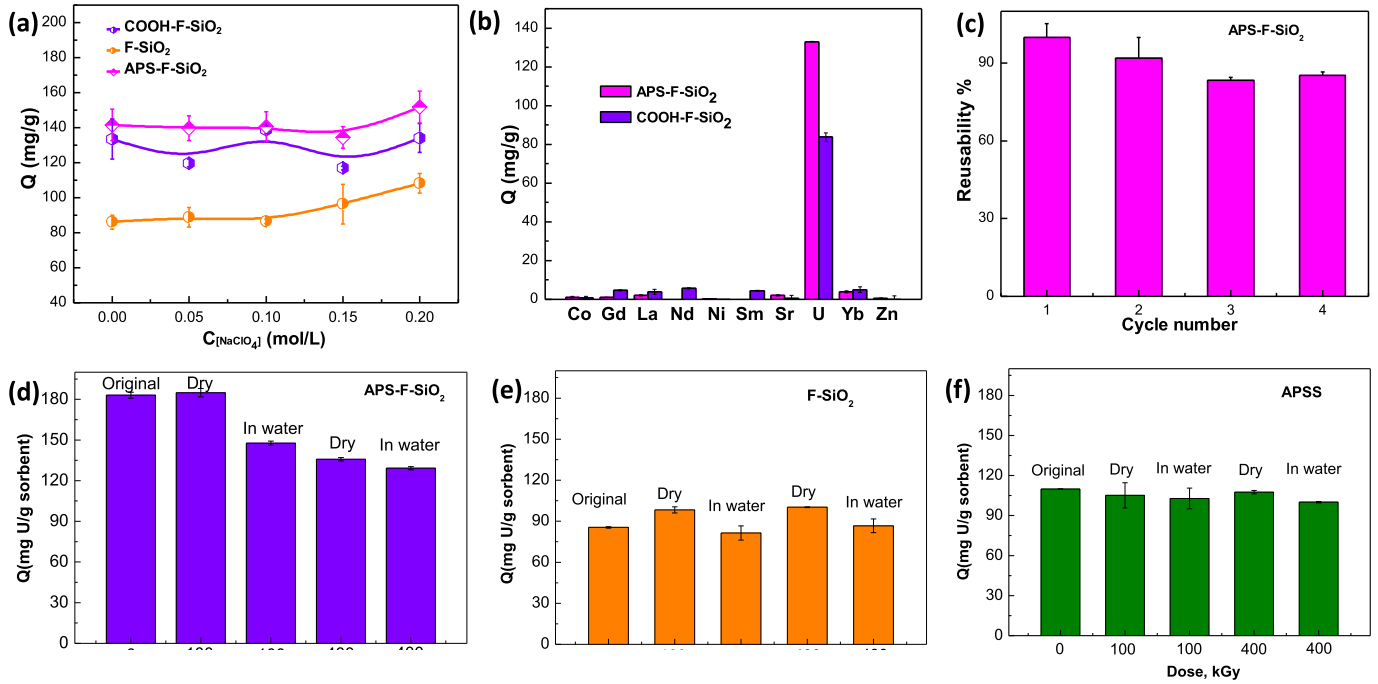

Fig. 3. (a) Effect of ionic strength on the sorption of U(VI) in F-SiO_2, APS-F-SiO_2 and COOH-F-SiO_2. $m_{sorbent}/V_{solution}$ = 0.4 mg mL^{-1}; $[U]_{initial}$ = 100 mg L^{-1}; pH = 5 ± 0.02; (b) Competitive sorption of U(VI) onto APS-F-SiO_2 and COOH-F-SiO_2. The concentration of all metal ion(s) was 0.65 mmol L^{-1}; (c) Reusability of APS-F-SiO_2 for U(VI) uptake. $[U]_{initial}$ = 100 mg L^{-1}, pH = 5, $m_{sorbent}/V_{solution}$ = 0.4 mg mL^{-1}; (d) Radiation stability of APS-F-SiO_2 for U(VI) uptake; (e) Radiation stability of pristine F-SiO_2 for U(VI) uptake; (f) Radiation stability of amine-grafted SBA-15 (APSS) for U(VI) uptake.

subjected to ^{60}Co gamma irradiation, respectively, and a dose rate of 60–80 Gy min^{-1} up to a maximum dose of 400 kGy was used. Then, the irradiated samples were used to sorb U(VI) from a fresh solution to assess the sorption stability. As can be seen from Fig. 3e, no discernable reduction of the U(VI) uptake for pristine F-SiO_2 were observed regardless of the irradiation conditions and doses, and there is even a slight enhancement of the U(VI) uptake for the dry samples probably due to the irradiation induced generation of surface defect and/or active site. For APS-F-SiO_2, however, the irradiation induced a certain reduction in the U(VI) uptake (Fig. 3d). At 400 kGy in water, for example, the U(VI) uptake is decreased from ca. 180 mg/g to ca. 130 mg/g. This reduction is undoubtedly related to the radiolysis of the amine groups on the silica beads. To further understand the radiolysis behavior, irradiation test of another kind of amine-grafted mesoporous silica, i.e. amine functionalized SBA-15 (APSS), was performed under exactly the same conditions. It is found that no decrease in the U(VI) sorption (Fig. 3f) occurred even following 400 kGy irradiation in water. At this point, we have come to the following conclusions: (1) the skeleton as well as the silanol of the pristine silica beads exhibit good stability towards gamma irradiation; (2) the radiation stability of the surface functional groups depends on the pore structure of the silica beads. Specially, less open pore structure in SBA-15 protects the amine groups from being ionized, whereas for F-SiO_2 more open pore structure has weak protection for functional groups, thus leading to the partial radiolysis of the amine groups. Whatever, even after 400 kGy irradiation in water, a high U(VI) uptake of 130 mg/g for APS-F-SiO_2 was maintained. This value is still larger than that for pristine F-SiO_2 and APSS. From this point of view, APS-F-SiO_2 is applicable in radionuclide capture from waste water.

4. Conclusions

A new family of actinide sorbents with more open porous structure was developed here by grafting a suite of functional groups, including amidoxime (AD-F-SiO_2), phosphate (DPTS-F-SiO_2), amino (APS-F-SiO_2), and carboxyl (COOH-F-SiO_2), onto fibrous mesoporous silica (F-SiO_2). The large pore channels of the fibrous mesoporous silicas not only avoid the clogging of the pores by the grafted functional group but also contribute to the diffusion of actinide ions therein, thus facilitating their real applications. Derived from the improvement of raw F-SiO_2, the functionalized materials became efficient, feasible and stable sorbents for U(VI) capture. The high-efficiency of the materials was demonstrated by the fast sorption kinetic of less than 30 min and the large sorption capacity as high as 200 mg/g at pH 5.0. Moreover, some of the sorbents (e.g COOH-F-SiO_2) show clear U(VI) sorption at pH as low as 2.5. In-depth studies indicated that the F-SiO_2 sorbents exhibit ionic strength-independent nature and desirable selectivity during the U(VI) sorption. The APS-F-SiO_2 sorbent remain high performance in U(VI) capture even following four sorption-desorption cycles or after 400 kGy irradiation in water. All these findings substantiate the applicability of these materials for U(VI) capture from wastewater. This work broadens a better horizon by introducing multifunctionality into fibrous mesoporous silica microsphere for the separation, removal, or recovery of actinides ions from environment. Further works are ongoing to fabricate more effective actinides sorbent by incorporating bulky organic ligands into fibrous mesoporous silicas for possible application in actinide and lanthanide separation.

Declaration of Competing Interest

The authors declare that they have no known competing financial interests or personal relationships that could have appeared to influence the work reported in this paper.

Acknowledgements

This work was supported by the National Natural Science Foundation of China (Grant No. 21777161, 21836001, 21577144 and 21806167) and Youth Innovation Promotion Association, CAS. The Science Challenge Project (TZ2016004) is also acknowledged.

Appendix A. Supplementary data

Supplementary data to this article can be found online at https://doi.org/10.1016/j.cej.2019.123892.

References

[1] Y.D. Zou, Y. Liu, X.X. Wang, G.D. Sheng, S.H. Wang, Y.J. Ai, Y.F. Ji, Y.H. Liu, T. Hayat, X.K. Wang, Glycerol-modified binary layered double hydroxide nanocomposites for uranium immobilization via extended X-ray absorption fine structure technique and density functional theory calculation, ACS Sustain. Chem. Eng. 5 (2017) 3583–3595.

[2] A. Bleise, P.R. Danesi, W. Burkart, Properties, use and health effects of depleted uranium (DU): a general overview, J. Environ. Radioact. 64 (2003) 93–112.

[3] Y. Dai, R. Lv, J. Fan, H. Peng, Z. Zhang, X. Cao, Y. Liu, Highly ordered macroporous silica dioxide framework embedded with supramolecular as robust recognition agent for removal of cesium, J. Hazard. Mater. (2019), https://doi.org/10.1016/j.jhazmat.2019.121467.

[4] J.H. Chiu, T.C. Chu, P.S. Weng, Radiochemical determination of Tc-99 in llw by chelation with sodium diethyl dithiocarbamate (naddc) and extraction with chloroform, J. Radioanal. Nucl. Chem. Art. 150 (1991) 493–507.

[5] Y.V. Nancharaiah, H.M. Joshi, T.V.K. Mohan, V.P. Venugopalan, S.V. Narasimhan, Aerobic granular biomass: a novel biomaterial for efficient uranium removal, Curr. Sci. 91 (2006) 503–509.

[6] H.B. Ortiz-Oliveros, R.M. Flores-Espinosa, H. Jimenez-Dominguez, M.C. Jimenez-Moleon, D. Cruz-Gonzalez, Dissolved air flotation for treating wastewater of the nuclear industry: preliminary results, J. Radioanal. Nucl. Chem. 292 (2012) 957–965.

[7] Z. Li, F. Chen, L. Yuan, Y. Liu, Y. Zhao, Z. Chai, W. Shi, Uranium(VI) adsorption on graphene oxide nanosheets from aqueous solutions, Chem. Eng. J. 210 (2012) 539–546.

[8] S.J. Yu, X.X. Wang, Y.F. Liu, Z.S. Chen, Y.H. Wu, Y. Liu, H.W. Pang, G. Song, J.R. Chen, X.K. Wang, Efficient removal of uranium(VI) by layered double hydroxides supported nanoscale zero-valent iron: a combined experimental and spectroscopic studies, Chem. Eng. J. 365 (2019) 51–59.

[9] H.W. Pang, Y.H. Wu, S.Y. Huang, C.C. Ding, S. Li, X.X. Wang, S.J. Yu, Z.S. Chen, G. Song, X.K. Wang, Macroscopic and microscopic investigation of uranium elimination by Ca-Mg-Al-layered double hydroxide supported nanoscale zero valent iron, Inorg. Chem. Front. 5 (2018) 2657–2665.

[10] S.J. Yu, D.L. Wei, L. Shi, Y.J. Ai, P. Zhang, X.X. Wang, Three-dimensional graphene/titanium dioxide composite for enhanced U(VI) capture: insights from batch experiments, XPS spectroscopy and DFT calculation, Environ. Pollut. 251 (2019) 975–983.

[11] Z.B. Zhang, Z.M. Dong, X.X. Wang, Y. Dai, X.H. Cao, Y.Q. Wang, R. Hua, H.T. Feng, J.R. Chen, Y.H. Liu, B.W. Hu, X.K. Wang, Synthesis of ultralight phosphorylated carbon aerogel for efficient removal of U(VI): batch and fixed-bed column studies, Chem. Eng. J. 370 (2019) 1376–1387.

[12] S.J. Yu, L. Yin, H.W. Pang, Y.H. Wu, X.X. Wang, P. Zhang, B.W. Hu, Z.S. Chen, X.K. Wang, Constructing sphere-like cobalt-molybdenum-nickel ternary hydroxide and calcined ternary oxide nanocomposites for efficient removal of U(VI) from aqueous solutions, Chem. Eng. J. 352 (2018) 360–370.

[13] L. Yuan, Y. Liu, W. Shi, Z. Li, J. Lan, Y. Feng, Y. Zhao, Y. Yuan, Z. Chai, A novel mesoporous material for uranium extraction, dihydroimidazole functionalized SBA-15, J. Mater. Chem. 22 (2012) 17019.

[14] H. Wu, Y. Shi, X. Guo, S. Zhao, J. Du, H. Jia, L. He, L. Du, Determination and removal of sulfonamides and quinolones from environmental water samples using magnetic adsorbents, J. Sep. Sci. 39 (2016) 4398–4407.

[15] X.W. Zeng, Y.G. Fan, G.L. Wu, C.H. Wang, R.F. Shi, Enhanced adsorption of phenol from water by a novel polar post-crosslinked polymeric adsorbent, J. Hazard. Mater. 169 (2009) 1022–1028.

[16] M.R. Awual, A novel facial composite adsorbent for enhanced copper(II) detection and removal from wastewater, Chem. Eng. J. 266 (2015) 368–375.

[17] Y. Sun, D. Shao, C. Chen, S. Yang, X. Wang, Highly efficient enrichment of radionuclides on graphene oxide-supported polyaniline, Environ. Sci. Technol. 47 (2013) 9904–9910.

[18] Z. Bai, L. Yuan, L. Zhu, Z. Liu, S. Chu, L. Zheng, J. Zhang, Z. Chai, W. Shi, Introduction of amino groups into acid-resistant MOFs for enhanced U(VI) sorption, J. Mater. Chem. A 3 (2015) 525–534.

[19] A. Afsar, L.M. Harwood, M.J. Hudson, P. Distler, J. John, Effective separation of Am (III) and Eu(III) from HNO_3 solutions using CyMe4-BTPhen-functionalized silica-coated magnetic nanoparticles, Chem. Commun. 50 (2014) 15082–15085.

[20] H.W. Pang, S.Y. Huang, Y.H. Wu, D.X. Yang, X.X. Wang, S.J. Yu, Z.S. Chen, A. Alsaedi, T. Hayat, X.K. Wang, Efficient elimination of U(VI) by polyethyleneimine-decorated fly ash, Inorg. Chem. Front. 5 (2018) 2399–2407.

[21] Y. Xie, J. Wang, M. Wang, X. Ge, Fabrication of fibrous amidoxime-functionalized mesoporous silica microsphere and its selectively adsorption property for Pb(2+) in aqueous solution, J. Hazard. Mater. 297 (2015) 66–73.

[22] L.Y. Yuan, Z.Q. Bai, R. Zhao, Y.L. Liu, Z.J. Li, S.Q. Chu, L.R. Zheng, J. Zhang, Y.L. Zhao, Z.F. Chai, W.Q. Shi, Introduction of bifunctional groups into mesoporous silica for enhancing uptake of thorium(IV) from aqueous solution, ACS Appl. Mater. Interfaces 6 (2014) 4786–4796.

[23] L.Y. Yuan, Y.L. Liu, W.Q. Shi, Y.L. Lv, J.H. Lan, Y.L. Zhao, Z.F. Chai, High performance of phosphonate-functionalized mesoporous silica for U(VI) sorption from aqueous solution, Dalton Trans. 40 (2011) 7446–7453.

[24] L.Y. Yuan, L. Zhu, C.L. Xiao, Q.Y. Wu, N. Zhang, J.P. Yu, Z.F. Chai, W.Q. Shi, Large-pore 3D cubic mesoporous (KIT-6) hybrid bearing a hard-soft donor combined ligand for enhancing U(VI) capture: an experimental and theoretical investigation, ACS Appl. Mater. Interfaces 9 (2017) 3774–3784.

[25] M. Zeng, Y. Huang, S. Zhang, S. Qin, J. Li, J. Xu, Removal of uranium(vi) from aqueous solution by magnetic yolk–shell iron oxide@magnesium silicate microspheres, RSC Adv. 4 (2014) 5021.

[26] N. Kothalawala, J.P. Blitz, V.M. Gun'ko, M. Jaroniec, B. Grabicka, R.F. Semeniuc, Post-synthesis surface-modified silicas as adsorbents for heavy metal ion contaminants Cd(II), Cu(II), Cr(III), and Sr(II) in aqueous solutions, J. Colloid Interface Sci. 392 (2013) 57–64.

[27] W. Li, D. Zhao, An overview of the synthesis of ordered mesoporous materials, Chem. Commun. 49 (2013) 943–946.

[28] F. Hoffmann, M. Cornelius, J. Morell, M. Froba, Silica-based mesoporous organic-inorganic hybrid materials, Angew. Chem. Int. Ed. Engl. 45 (2006) 3216–3251.

[29] Z. Wang, C. Xu, Y. Lu, F. Wu, G. Ye, G. Wei, T. Sun, J. Chen, Visualization of adsorption: luminescent mesoporous silica-carbon dots composite for rapid and selective removal of U(VI) and in situ monitoring the adsorption behavior, ACS Appl. Mater. Interfaces 9 (2017) 7392–7398.

[30] D. Li, S. Egodawatte, D.I. Kaplan, S.C. Larsen, S.M. Serkiz, J.C. Seaman, Functionalized magnetic mesoporous silica nanoparticles for U removal from low and high pH groundwater, J. Hazard. Mater. 317 (2016) 494–502.

[31] Y. Liu, L. Yuan, Y. Yuan, J. Lan, Z. Li, Y. Feng, Y. Zhao, Z. Chai, W. Shi, A high efficient sorption of U(VI) from aqueous solution using amino-functionalized SBA-15, J. Radioanal. Nucl. Chem. 292 (2012) 803–810.

[32] V. Polshettiwar, D. Cha, X. Zhang, J.M. Basset, High-surface-area silica nanospheres (KCC-1) with a fibrous morphology, Angew. Chem. Int. Ed. Engl. 49 (2010) 9652–9656.

[33] J. Chen, S. Lei, Y. Xie, M. Wang, J. Yang, X. Ge, Fabrication of high-performance magnetic lysozyme-imprinted microsphere and its NIR-responsive controlled release property, ACS Appl. Mater. Interfaces 7 (2015) 28606–28615.

[34] S.L. Gai, P.P. Yang, P.A. Ma, D. Wang, C.X. Li, X.B. Li, N. Niu, J. Lin, Fibrous-structured magnetic and mesoporous Fe3O4/silica microspheres: synthesis and intracellular doxorubicin delivery, J. Mater. Chem. 21 (2011) 16420–16426.

[35] K. Vidya, S. Dapurkar, P. Selvam, S. Badamali, N. Gupta, The entrapment of UO_2^{2+} in mesoporous MCM-41 and MCM-48 molecular sieves, Microporous Mesoporous Mater. 50 (2001) 173–179.

[36] J.H. Kim, H.I. Lee, J.-W. Yeon, Y. Jung, J.M. Kim, Removal of uranium(VI) from aqueous solutions by nanoporous carbon and its chelating polymer composite, J. Radioanal. Nucl. Chem. 286 (2010) 129–133.

[37] D. Shao, Z. Jiang, X. Wang, J. Li, Y. Meng, Plasma induced grafting carboxymethyl cellulose on multiwalled carbon nanotubes for the removal of UO22+ from aqueous solution, J. Phys. Chem. B 113 (2009) 860–864.

[38] R.M. Barrer, S. Barri, J. Klinowski, Zeolite rho. 2. cation-exchange equilibria and kinetics, J. Chem. Soc., Faraday Trans. I 76 (1980) 1038–1051.

[39] C. Kantipuly, S. Katragadda, A. Chow, H. Gesser, Chelating polymers and related supports for separation and preconcentration of trace metals, Talanta 37 (1990) 491–517.

[40] D.M. Singer, K. Maher, G.E. Brown, Uranyl–chlorite sorption/desorption: evaluation of different U (VI) sequestration processes, Geochim. Cosmochim. Acta 73 (2009) 5989–6007.

[41] C.R. Preetha, J.M. Gladis, T.P. Rao, G. Venkateswaran, Removal of toxic uranium from synthetic nuclear power reactor effluents using uranyl ion imprinted polymer particles, Environ. Sci. Technol. 40 (2006) 3070–3074.